

Quantum Griffiths Phase in the weak itinerant ferromagnetic alloy $\text{Ni}_{1-x}\text{V}_x$

Sara Ubaid-Kassis,¹ Thomas Vojta,² and Almut Schroeder¹

¹*Physics Department, Kent State University, Kent OH 44242*

²*Department of Physics, Missouri University of Science and Technology, Rolla, MO 65409*

(Dated: July 15, 2021)

We present magnetization (M) data of the d -metal alloy $\text{Ni}_{1-x}\text{V}_x$ at vanadium concentrations close to $x_c \approx 11.4\%$ where the onset of long-range ferromagnetic (FM) order is suppressed to zero temperature. Above x_c , the temperature (T) and magnetic field (H) dependencies of the magnetization are best described by simple nonuniversal power laws. The exponents of $M/H \sim T^{-\gamma}$ and $M \sim H^\alpha$ are related by $1 - \gamma = \alpha$ for wide temperature ($10\text{K} < T \leq 300\text{K}$) and field ($H \leq 5T$) ranges. γ is strongly x dependent, decreasing from 1 at $x \approx x_c$ to $\gamma < 0.1$ for $x=15\%$. This behavior is not compatible with either classical or quantum critical behavior in a clean 3D FM. Instead it closely follows the predictions for a quantum Griffiths phase associated with a quantum phase transition in a disordered metal. Deviations at the lowest temperatures hint at a freezing of large clusters and the onset of a cluster glass phase, presumably due to RKKY interactions in this alloy.

PACS numbers: 71.27.+a, 75.40.-s, 75.50.Cc

Magnetic phase transitions in metals continue to offer challenges to theory and experiment. In recent years, the focus has shifted from thermal transitions (such as the onset of ferromagnetism in nickel at a temperature of 630K [1]) to quantum phase transitions (QPTs) [2] that occur at zero temperature when a parameter such as pressure or chemical composition is varied. Spin fluctuations associated with continuous QPTs or quantum critical points (QCPs) are believed to be responsible for a variety of exotic phenomena including deviations from the fundamental Fermi liquid behavior of normal metals.

Ferromagnetic and antiferromagnetic QCPs have been observed in transition metal alloys and heavy-fermion compounds (see Ref. [3] for a review). Quantum critical behavior is signified by singularities in thermodynamic and transport properties. According to the standard theory of ferromagnetic quantum criticality in 3D metals [4], specific heat C , magnetic susceptibility χ and electrical resistivity ρ should behave as $\chi \sim T^{-4/3}$, $C/T \sim \log(T)$ and $\rho(T) \sim T^{5/3}$ when approaching the QCP at low temperatures T . This was observed in $\text{Ni}_x\text{Pd}_{1-x}$ with $x = 0.025$, at least over a limited temperature regime [5]. However, most “clean” weak ferromagnets like MnSi [6], ZrZn_2 [7] or Ni_3Al [8] show deviations from the above predictions. The QPT becomes first order [9] and is often accompanied by the appearance of novel phases.

Many ferromagnetic binary alloys such as $\text{Ni}_{1-x}\text{Cu}_x$ or $\text{Ni}_{1-x}\text{V}_x$ in which T_c can be tuned by chemical substitution x show a still more complicated behavior, even in the paramagnetic phase. In early investigations [10], the existence of large magnetic clusters with giant local moments was proposed to describe the magnetization M data of these inhomogeneous systems.

Recent theories address the impact of disorder on QPTs more systematically (for a review, see Ref. [11]). We are interested in the case of metallic (itinerant) Heisenberg magnets. For these systems a strong-disorder renormalization group [12] predicts an exotic infinite-randomness QCP, accompanied by quantum Griffiths sin-

gularities [13]. At such a QCP, thermodynamic observables are expected to be singular not just at criticality but in a finite region around the QCP called the Griffiths phase. This is caused by rare spatial regions that are locally in the magnetic phase while the bulk is still nonmagnetic. The probability w of finding such regions is exponentially small in their volume V , $w \sim \exp(-bV)$ with b a constant that depends on the disorder strength. Importantly, the characteristic energy scale ϵ of a locally ordered region also depends exponentially on its volume, $\epsilon \sim \exp(-cV)$. Combining these two exponentials yields an energy spectrum $P(\epsilon) \sim \epsilon^{\lambda-1}$. The nonuniversal Griffiths exponent $\lambda = b/c$ takes the value 0 at the quantum critical point and increases with distance from criticality. This power-law spectrum gives rise to power-law quantum Griffiths singularities of many observables, including specific heat $C \sim T^\lambda$, susceptibility $\chi \sim T^{\lambda-1}$ and the zero temperature magnetization-field curve, $M \sim H^\lambda$.

Quantum Griffiths singularities have attracted a lot of attention, but clearcut experimental verifications have been slow to arrive. Many heavy fermion compounds display anomalous power-laws in $C(T)$ and $\chi(T)$ [14]; and quantum Griffiths behavior was suggested as an explanation [15]. However, in most of these systems, a systematic variation of the exponents in accordance with theory could not be observed. Only recently, a partial confirmation could be found at the ferromagnetic QPT of $\text{CePd}_{1-x}\text{Rh}_x$ [16]. It must also be noted that the interpretation of experiments in heavy-fermion compounds suffers from additional complications due to the Kondo effect which plays a crucial role for the magnetic properties. It is thus highly desirable to observe quantum Griffiths singularities in a simpler system.

In this Letter we therefore study the transition metal alloy $\text{Ni}_{1-x}\text{V}_x$ as an example of an itinerant ferromagnet in which T_c can be tuned to zero by chemical substitution while introducing strong disorder. We show that magnetization and susceptibility close to the critical vanadium concentration indeed follow the quantum Griffiths sce-

arXiv:0912.1146v2 [cond-mat.str-el] 23 Mar 2010

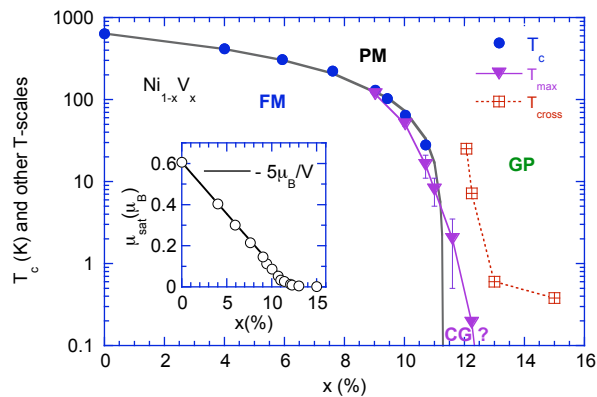


FIG. 1: Temperature-concentration phase diagram of $\text{Ni}_{1-x}\text{V}_x$ showing ferromagnetic (FM), paramagnetic (PM), quantum Griffiths (GP), and cluster glass (CG) phases. Circles mark T_c found via the Arrott analysis. The grey line is an extrapolation of $T_c(x)$. Also shown are T_{max} defined by low-field maxima in $\chi(T)$ and T_{cross} below which frozen clusters dominate $\chi(T)$, leading to superparamagnetism. Inset: saturation magnetization μ_{sat} vs x (determined as $M(T < 5\text{K}, H > 1\text{T})$). Data from Ref. [17] for $x < 11\%$ are included.

nario over a wide temperature and magnetic field range.

Polycrystalline spherical $\text{Ni}_{1-x}\text{V}_x$ samples with $x = 9 - 15\%$ were prepared by arc melting from high purity elements (Ni 99.995%, V 99.8%) and annealed at 900 - 1050°C. X-ray diffraction confirmed a single phase fcc-structure with lattice constant $a = (0.352 + 0.023x)\text{nm}$. Magnetization measurements were performed in a Quantum Design SQUID magnetometer from 1.8K - 300K and magnetic fields up to 5T. The ac-susceptibility was measured in a pick up coil in a dilution refrigerator down to 0.05K and calibrated through the overlap with the magnetometer data. All data shown are demagnetized.

It is known that T_c of $\text{Ni}_{1-x}\text{V}_x$ is rapidly reduced with increasing V-concentration x [17]. As explained by Friedel [18], $\text{Ni}_{1-x}\text{V}_x$ resides on a side branch of the Slater-Pauling curve: a V impurity (with 5 fewer electrons than Ni) creates a localized charge and a spin reduction on the neighboring Ni-sites. This reduces the average spin moment by $5\mu_B/V$ from $0.6\mu_B/\text{Ni}$ leading to a critical concentration of about 12%. It also creates large defects yielding an inhomogeneous magnetization density which makes $\text{Ni}_{1-x}\text{V}_x$ an ideal compound to study a QPT with significant “disorder”.

The phase diagram resulting from our measurements is shown in Fig. 1. To get an overview, we first perform a standard Arrott analysis. Samples with $x \leq 11\%$ show mean-field behavior, i.e., parallel isotherms of the form $H/M = a + bM^2$ as is common for itinerant magnets. (Mean-field behavior is expected outside the actual critical region; if the standard theory [4] applied, it would describe the entire transition up to log. corrections.) T_c is extracted from the Arrott plots via the mean-field T -dependencies of magnetization and susceptibility.

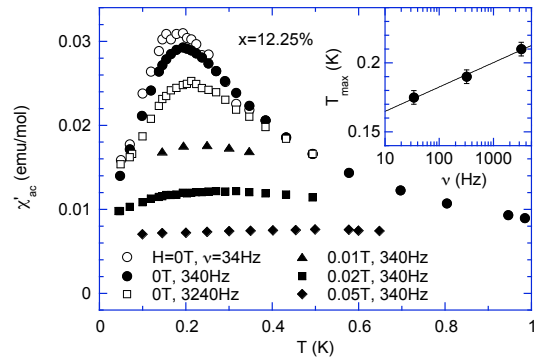


FIG. 2: ac-susceptibility χ_{ac} of the $x = 12.25\%$ sample for several dc magnetic fields H and frequencies ν of the (in phase) ac-magnetic field ($H_{ac} \approx 0.1\text{G}$) vs temperature T . Inset shows the frequency dependence of the maximum in $\chi(T)$ T_{max} . The line follows $dT_{max}/d(\log \nu) = 0.018\text{K}/\text{dec}(\nu)$.

For $x > 11\%$, clear deviations from mean-field behavior (linear Arrott plots) [19]; and the determination of T_c becomes sensitive to model assumptions. In addition to Arrott plots, we analyze the differential susceptibility $\chi(T) = dM(T)/dH$. It exhibits a field-dependent maximum at $T_{max}(H)$, indicating spin ordering or freezing. Figure 1 shows $T_{max}(H \rightarrow 0)$ estimated by a linear extrapolation of the data taken at 0.5T to 0.1T. $T_{max}(H \rightarrow 0)$ is somewhat lower than T_c derived from the high field mean field analysis. We note that the magnetization for $x > 11\%$ and higher fields $H > 0.5\text{T}$ can be described by parallel isotherms in a modified Arrott plot [20] ($(H/M)^{(1/\gamma)} = a + bM^{(1/\beta)}$) with exponents $\beta = 0.5$ and an x -dependent $\gamma(x) < 1$ [19]. However, this yields a finite T_c well above T_{max} for all $x \leq 15\%$.

Within our error bars, $T_{max}(H \rightarrow 0)$ is definitely nonzero for $x \leq 11\%$ but zero for $x \geq 13\%$. To understand the behavior at intermediate concentrations, we measure the ac-susceptibility χ_{ac} in a small ac-field $H_{ac} \approx 0.1\text{G}$ down to 50mK as shown in Fig. 2 for the sample with $x = 12.25\%$. A maximum in $\chi_{ac}(T)$ at $T_{max} = 0.19\text{K}$ marks spin freezing in 0mT at a low frequency of $\nu = 340\text{Hz}$. It is rapidly suppressed in small dc-fields and shifted to higher T . T_{max} is dependent on ν like in a spin glass, signifying irreversibility in this system. At higher T , no significant hysteresis in $M(H)$ was found for all samples with a remanent field larger than the rest field of the magnet of the order of 10G.

We emphasize that deviations from linear Arrott plots and the sensitivity of T_c towards the extrapolation procedure already point to an unconventional QPT. Moreover, the x -dependence of $T_{max}(H \rightarrow 0)$ in the accessible temperature region is better described by an exponential rather than a power law, making the determination of the x_c from finite-temperature data difficult.

We now turn to the paramagnetic phase above the critical concentration $x_c \approx 11\%$. In the past, the susceptibility at higher temperatures ($T > 40\text{K}$) has been described

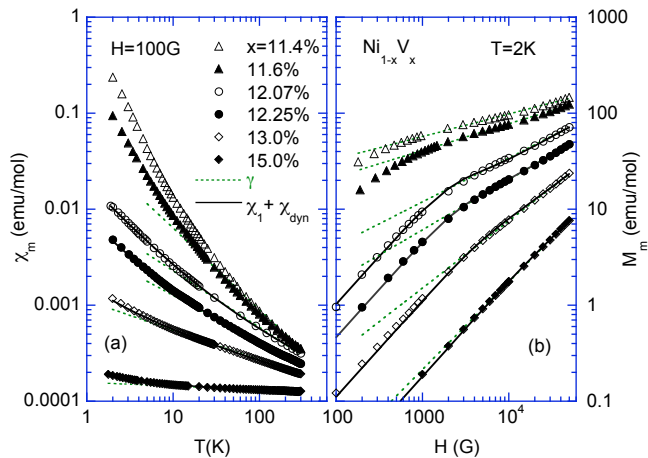


FIG. 3: (a) Low-field susceptibility $\chi_m = M/H - \chi_{orb}$ of $\text{Ni}_{1-x}\text{V}_x$ vs temperature T and (b) low-temperature magnetization $M_m = M - \chi_{orb}H$ vs magnetic field H ($x = 11-15\%$). Dotted lines indicate power laws for $T > 10$ K and $H > 3000$ G in (a) and (b), respectively. Solid lines (shown for $x > 12\%$) represent fits to the model (2) with frozen clusters.

[10] by a Curie-Weiss law $\chi = C/(T - \theta) + \chi_{orb}$, but this only works if the orbital contribution χ_{orb} is allowed to vary by a factor of 3 with concentration x . In our analysis, we keep the orbital susceptibility x -independent at $\chi_{orb} = 6 \times 10^{-5}$ emu/mol which is the best fit parameter for $x < x_c$ and lies within the reported estimates [21].

The resulting low-field ($H = 100$ G) spin susceptibility $\chi_m = M/H - \chi_{orb}$ is shown in Fig. 3a for samples with $x = 11 - 15\%$. At temperatures above 10 K, simple power laws describes the data well. We parametrize the power law by $\chi_m(T) = A(k_B T)^{-\gamma}$. The exponent γ is determined from fits between 30K and 300K (300K may seem a very high temperature for analyzing a QPT, but it is still well below the Curie point of Nickel at 630K; this high bare temperature scale is another advantage of our material.) Figure 4a shows that γ varies from about 1 for $x = 11.4\%$ towards 0.03 for $x = 15\%$. We also analyze the magnetization-field curve. Figure 3b shows $M_m = M - \chi_{orb}H$ as a function of field at the lowest $T = 2$ K for samples with $x > 11\%$. For fields above $H > 3000$ G $\approx k_B T / 10 \mu_B$, $M(H)$ follows a power law with an exponent α . Its value (shown in Fig. 4a) matches the susceptibility exponent, $1 - \alpha = \gamma$ for $x > 12\%$.

The results for $\chi_m(T)$ and $M_m(H)$ are in excellent agreement with the predictions for a quantum Griffiths phase outlined in the introduction if we identify the Griffiths exponent via $\lambda = \alpha = 1 - \gamma$. The critical concentration x_c can now be determined from the condition $\lambda = 0$ which gives $x_c \approx 11.4\%$ using the susceptibility data. Right at criticality, the theory [12] predicts extra logarithmic corrections (which are notoriously hard to verify) to the power laws. Our fits did not noticeably improve by including logarithmic terms.

To combine the temperature and field dependencies (at

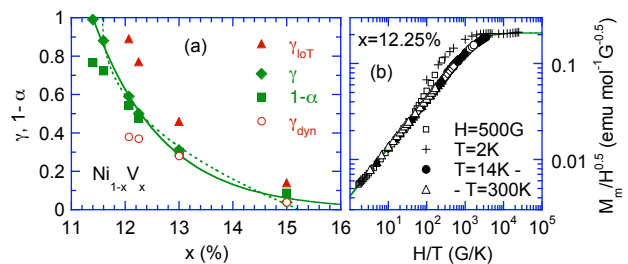


FIG. 4: (a) Exponents $\gamma, 1 - \alpha$ obtained from $\chi_m \sim T^\gamma$ and $M_m \sim H^\alpha$ vs V-concentration x . The plot also shows γ_{loT} derived from $\chi_m(T)$ below 10 K and γ_{dyn} extracted from the fit to (2). The x -dependence of γ can be fitted to a power law, $(1 - \gamma) \sim (x - x_c)^{\nu\psi}$ (dotted line), as expected according to [12] (with $\nu\psi \approx 0.42$) or to an exponential, $-\ln \gamma \sim (x - x_c)$ (solid line). (b) H/T scaling plot for $x = 12.25\%$ showing data at several const. T from 2K - 300K and $H = 500$ G. The line is a fit to the phenomenological form discussed below (1).

fixed x) of the magnetization we suggest the scaling form

$$M = H^\alpha Y(\mu H / k_B T) \quad (1)$$

where Y is the scaling function and μ is a scaling moment. The corresponding scaling plot for $x = 12.25\%$ is shown in Fig. 4b. All $M(H, T)$ data for temperatures above 14 K collapse, confirming H/T scaling. The scaling function Y is well approximated by the phenomenological form $Y(z) = A' / (1 + z^{-2})^{\gamma/2}$ where $A' = A / \mu^\gamma$ is a constant. We have produced similar scaling plots for the other concentrations. The resulting exponent γ matches that obtained by a direct fit of $\chi(T)$ for all x between 11.4% and 15%. The scaling moment μ increases from $1\mu_B$ at $x = 15\%$ to $12\mu_B$ at $x = 11.4\%$ demonstrating the growth of the typical cluster size with $x \rightarrow x_c$ [22]. An analogous scaling form was used to describe the H/T scaling in heavy fermions [23]. It also gives the correct exponent for the nonlinear susceptibility ($\chi_3 = d(M/H)/d(H^2) \sim T^{\alpha-3}$ for $T \gg H$).

Having established the quantum Griffiths phase, we now turn to its limits. At $T < 10$ K, deviations are observed from the ‘‘Griffiths’’ power laws. For instance, γ increases by about 50% (see Fig. 4). This exponent does not match $1 - \alpha$. We thus believe that the behavior below 10K deviates from the quantum Griffiths scenario either due to the Vanadium distribution not being perfectly statistical or because the rare regions are not independent.

It was shown [25] that RKKY interactions between the rare regions lead to a dynamical freezing of the largest clusters at low T and to the formation of a cluster glass at even lower T . To explore this possibility, we model the zero-field susceptibility

$$\chi_m(T) = \chi_1 + \chi_{dyn} = A_1 / (k_B T) + A / (k_B T)^{\gamma_{dyn}} \quad (2)$$

as the sum of a Curie term χ_1 (describing the frozen clusters) and a Griffiths term with an exponent γ_{dyn} . This model describes the data in Fig. 3a over the entire

temperature region above T_{max} . A similar model can be formulated for the magnetization-field data in Fig. 3b.

We define a crossover temperature T_{cross} as the temperature where χ_1 exceeds χ_{dyn} (see Fig. 1). It can be regarded as the boundary of the Griffiths phase. For $x = 12.25\%$, $T_{cross} \approx 7\text{K}$ which is much higher than the cluster glass temperature 0.19K found via the ac-susceptibility. This leaves room for a significant superparamagnetic regime where independent frozen clusters dominate. We note that superparamagnetism can arise in systems with Ising spin symmetry even without rare region interactions [26]. However, our system does not show any indications of reduced spin symmetry.

Further analysis of the Curie term requires insight into the structure of the rare region interactions. In a purely percolative scenario, one expects $A_1 \sim |x - x_c|^{-\gamma_c}$ with the percolation exponent $\gamma_c = 1.8$. Our data indeed show a divergence of A_1 with $x \rightarrow x_c$ but with an exponent of about 2.6. Alternatively, one can successfully model the Curie term as a contribution from a number of frozen clusters of fixed moment which increases from $2\mu_B$ for $x = 15\%$ to $15\mu_B$ for $x = 12.07\%$ as x_c is approached. A more detailed discussion will be published elsewhere.

We emphasize that the theory [12, 13] for quantum Griffiths effects in metals was originally developed for antiferromagnets rather than ferromagnets. In ferromagnets, mode-coupling effects produce an additional long-range interaction [9] which renders the disorder perturbatively irrelevant at the clean QCP [27]. However, this

does not preclude the existence of Griffiths singularities because they are nonperturbative degrees of freedom. In fact, it was recently shown [28] that the physics of independent rare regions in a ferromagnet is the same as in an antiferromagnet. We thus believe that the quantum Griffiths scenario is applicable to our system, at least above the crossover temperature where interactions between rare regions become important [29].

In summary, we have presented magnetization and susceptibility measurements of the transition metal alloy $\text{Ni}_{1-x}\text{V}_x$ close to the critical concentration for the onset of ferromagnetism. While the finite-temperature phase transition in the concentrated Ni regime ($x \leq 11\%$) is well described by mean-field behavior, the diluted regime with low or vanishing T_c cannot be described in terms of conventional critical behavior. Instead, the data follow the predictions of a quantum Griffiths phase associated with an infinite-randomness QCP over a wide temperature and field region. Previous specific heat [24] and transport data [10] support this scenario via anomalous power laws in a wide concentration range (even though they were not discussed in terms of a Griffiths phase). Deviations at lower T hint at individual freezing of large clusters before the system enters a cluster glass phase.

We thank C. C. Almasan and S. D. Huang for the use of the SQUID magnetometer and the X-ray diffractometer, respectively. This work has been supported in part by the NSF under grant nos. DMR-0306766, DMR-0339147, and DMR-0906566 as well as by Research Corporation

-
- [1] P. Weiss and R. Forrer, *Ann. Phys. (Paris)* **5**, 153 (1926).
 [2] S. Sachdev, *Quantum Phase Transitions* (Cambridge University Press, 1999).
 [3] H. v. Löhneysen, A. Rosch, M. Vojta, and P. Wölfle, *Rev. Mod. Phys.* **79**, 1015 (2007), and refs therein.
 [4] J. Hertz, *Phys. Rev. B* **14**, 1165 (1976); A.J. Millis, *Phys. Rev. B* **48**, 7183 (1993).
 [5] M. Nicklas *et al.*, *Phys. Rev. Lett.* **82**, 4268 (1999).
 [6] C. Pfeleiderer, G. J. McMullan, S. R. Julian, and G. G. Lonzarich, *Phys. Rev. B* **55**, 8330 (1997).
 [7] M. Uhlarz, C. Pfeleiderer, and S. M. Hayden, *Phys. Rev. Lett.* **93**, 256404 (2004).
 [8] P. G. Niklowitz, *et al.*, *Phys. Rev. B* **72**, 024424 (2005).
 [9] D. Belitz, T.R. Kirkpatrick and T. Vojta, *Phys. Rev. Lett.* **82**, 4707 (1999); *Rev. Mod. Phys.* **77**, 579 (2005).
 [10] A. Amamou, F. Gautier, and B. Loegel, *J. Phys. F: Met. Phys.* **5**, 1342 (1975).
 [11] T. Vojta, *J. Phys. A: Math Gen.* **39**, R143 (2006).
 [12] J.A. Hoyos, C. Kotabage, and T. Vojta, *Phys. Rev. Lett.* **99**, 230601 (2007); T. Vojta, C. Kotabage, and J. A. Hoyos, *Phys. Rev. B* **79**, 024401 (2009).
 [13] T. Vojta and J. Schmalian, *Phys. Rev. B* **72**, 045438 (2005).
 [14] G. R. Stewart, *Rev. Mod. Phys.* **73**, 797 (2001); G. R. Stewart, *Rev. Mod. Phys.* **78**, 743 (2006).
 [15] A. H. Castro Neto and B. A. Jones, *Phys. Rev. B* **62**, 14975 (2000).
 [16] T. Westerkamp *et al.*, *Phys. Rev. Lett.* **102**, 206404 (2009).
 [17] F. Bölling, *Phys. Kondens. Mater.* **7**, 162 (1968).
 [18] J. Friedel, *Nuovo Cimento* **7**, 287 (1958).
 [19] S. Ubaid-Kassis and A. Schroeder, *Physica B* **403**, 1325 (2008);
 [20] A. Arrott and J. E. Noakes, *Phys. Rev. Lett.* **19**, 786 (1967).
 [21] M. Shimizu, *Proc. Phys. Soc.* **84**, 397 (1964).
 [22] According to the theory [12], the typical moment should depend on temperature, but only very weakly (logarithmically) which is hard to confirm in any experiment.
 [23] A. Schröder, *et al.*, *Nature* **407**, 351 (2000).
 [24] I. P. Gregory and D. E. Moody, *J. Phys. F: Met. Phys.* **5**, 36 (1975).
 [25] V. Dobrosavljević and E. Miranda, *Phys. Rev. Lett.* **94**, 187203 (2005).
 [26] A. J. Millis, D. K. Morr, and J. Schmalian, *Phys. Rev. B* **66**, 174433 (2002); T. Vojta, *Phys. Rev. Lett.* **90**, 107202 (2003); J.A. Hoyos and T. Vojta, *Phys. Rev. Lett.* **100**, 240601 (2008).
 [27] R. Narayanan, T. Vojta, D. Belitz, and T.R. Kirkpatrick, *Phys. Rev. Lett.* **82**, 5132 (1999); *Phys. Rev. B* **60**, 10150 (1999).
 [28] J.A. Hoyos and T. Vojta, *Phys. Rev. B* **75**, 104418 (2007).
 [29] This implies that a complete renormalization group theory of the itinerant ferromagnetic QPT would have to include the nonperturbative degrees of freedom.